

Biomass resilience of Neotropical secondary forests

Lourens Poorter¹, Frans Bongers¹, T. Mitchell Aide², Angélica M. Almeyda Zambrano³, Patricia Balvanera⁴, Justin M. Becknell⁵, Vanessa Boukili⁶, Pedro H. S. Brancalion⁷, Eben N. Broadbent³, Robin L. Chazdon⁶, Dylan Craven^{8,9,10}, Jarcilene S. de Almeida-Cortez¹¹, George A. L. Cabral¹¹, Ben H. J. de Jong¹², Julie S. Denslow¹³, Daisy H. Dent^{14,15}, Saara J. DeWalt¹⁶, Juan M. Dupuy¹⁷, Sandra M. Durán¹⁸, Mario M. Espírito-Santo¹⁹, María C. Fandino²⁰, Ricardo G. César⁷, Jefferson S. Hall⁸, José Luis Hernández-Stefanoni¹⁷, Catarina C. Jakovac^{1,21}, André B. Junqueira^{22,23,24}, Deborah Kennard²⁵, Susan G. Letcher²⁶, Juan-Carlos Licona²⁷, Madelon Lohbeck^{1,28}, Erika Marín-Spiotta²⁹, Miguel Martínez-Ramos⁴, Paulo Massoca²¹, Jorge A. Meave³⁰, Rita Mesquita²¹, Francisco Mora^{4,30}, Rodrigo Muñoz³⁰, Robert Muscarella^{31,32}, Yule R. F. Nunes¹⁹, Susana Ochoa-Gaona¹², Alexandre A. de Oliveira³³, Edith Orihuela-Belmonte¹², Marielos Peña-Claros¹, Eduardo A. Pérez-García³⁰, Daniel Piotta³⁴, Jennifer S. Powers^{35,36}, Jorge Rodríguez-Velázquez⁴, I. Eunice Romero-Pérez³⁰, Jorge Ruiz^{37,38}, Juan G. Saldarriaga³⁹, Arturo Sanchez-Azofeifa¹⁸, Naomi B. Schwartz⁴⁰, Marc K. Steininger⁴⁰, Nathan G. Swenson⁴¹, Marisol Toledo²⁷, Maria Uriarte³¹, Michiel van Breugel^{8,42,43}, Hans van der Wal⁴⁴, Maria D. M. Veloso¹⁹, Hans F. M. Vester^{45,46}, Alberto Vicentini²¹, Ima C. G. Vieira⁴⁷, Tony Vizcarra Bentos²¹, G. Bruce Williamson^{21,48} & Danaë M. A. Rozendaal^{1,6,49}

Land-use change occurs nowhere more rapidly than in the tropics, where the imbalance between deforestation and forest regrowth has large consequences for the global carbon cycle¹. However, considerable uncertainty remains about the rate of biomass recovery in secondary forests, and how these rates are influenced by climate, landscape, and prior land use²⁻⁴. Here we analyse aboveground biomass recovery during secondary succession in 45 forest sites and about 1,500 forest plots covering the major environmental gradients in the Neotropics. The studied secondary forests are highly productive and resilient. Aboveground biomass recovery after 20 years was on average 122 megagrams per hectare (Mg ha^{-1}), corresponding to a net carbon uptake of $3.05 \text{ Mg C ha}^{-1} \text{ yr}^{-1}$, 11 times the uptake rate of old-growth forests. Aboveground biomass stocks took a median time of 66 years to recover to 90% of old-growth values. Aboveground biomass recovery after 20 years varied 11.3-fold (from 20 to 225 Mg ha^{-1}) across sites, and this recovery increased with water availability (higher local rainfall and lower climatic water deficit). We present a biomass recovery map of Latin America, which illustrates geographical and climatic variation

in carbon sequestration potential during forest regrowth. The map will support policies to minimize forest loss in areas where biomass resilience is naturally low (such as seasonally dry forest regions) and promote forest regeneration and restoration in humid tropical lowland areas with high biomass resilience.

Over half of the world's tropical forests are not old-growth, but naturally regenerating forests⁵. We focus here on secondary forests that regrow after nearly complete removal of forest cover for agricultural use⁴. Despite their crucial role in human-modified tropical landscapes, the rate at which these forests will recover, and the extent to which they can provide equivalent levels of ecosystem services as the forests they replaced, remains uncertain. Several studies suggest that, once a certain threshold of disturbance has been reached, tropical forests may collapse⁶ or switch to an alternative stable state⁷. However, in general, secondary tropical forests have rapid rates of carbon sequestration, with potentially large consequences for the global carbon cycle³. The magnitude of the tropical carbon sink is relatively well known for old-growth forest^{8,9}, but current global estimates on carbon uptake and storage of secondary forests are rough

¹Forest Ecology and Forest Management Group, Wageningen University, PO Box 47, 6700 AA Wageningen, The Netherlands. ²PO Box 23360, Department of Biology, University of Puerto Rico, San Juan, PR 00931-3360, Puerto Rico. ³Spatial Ecology and Conservation Lab, Department of Geography, University of Alabama, Tuscaloosa, Alabama 35487, USA. ⁴Instituto de Investigaciones en Ecosistemas y Sustentabilidad, Universidad Nacional Autónoma de México, CP58190, Morelia, Michoacán, México. ⁵Department of Ecology and Evolutionary Biology, Brown University, Providence, Rhode Island 02912, USA. ⁶Department of Ecology and Evolutionary Biology, University of Connecticut, Storrs, Connecticut 06269, USA. ⁷Department of Forest Sciences, Luiz de Queiroz College of Agriculture, University of São Paulo, Avenida Pádua Dias 11, 13418-900, Piracicaba, São Paulo, Brazil. ⁸SI ForestGEO, Smithsonian Tropical Research Institute, Roosevelt Avenue, Tupper Building - 401, Balboa, Ancón, Panamá, Panamá. ⁹German Centre for Integrative Biodiversity Research (iDiv) Halle-Jena-Leipzig, Deutscher Platz 5e, 04103 Leipzig, Germany. ¹⁰Institute for Biology, Leipzig University, Johannisallee 21, 04103 Leipzig, Germany. ¹¹Departamento de Botânica, Universidade Federal de Pernambuco, Pernambuco, CEP 50670-901, Brazil. ¹²Department of Sustainability Science, El Colegio de la Frontera Sur, Unidad Campeche, Av. Rancho Polígono 2A, Parque Industrial Lerma, Campeche, Campeche, CP 24500, México. ¹³Department of Ecology and Evolutionary Biology, Tulane University, New Orleans, Louisiana 70130, USA. ¹⁴Smithsonian Tropical Research Institute, Roosevelt Avenue, Tupper Building - 401, Balboa, Ancón, Panamá, Panamá. ¹⁵Biological and Environmental Sciences, University of Stirling, Stirling FK9 4LA, UK. ¹⁶Department of Biological Sciences, Clemson University, 132 Long Hall, Clemson, South Carolina 29634, USA. ¹⁷Centro de Investigación Científica de Yucatán, AC, Unidad de Recursos Naturales, Calle 43 No. 130, Colonia Chuburná de Hidalgo, CP 97200, Mérida, Yucatán, México. ¹⁸Earth and Atmospheric Sciences Department, University of Alberta, Edmonton, Alberta T6G 2E3, Canada. ¹⁹Departamento de Biología Geral, Universidade Estadual de Montes Claros, Montes Claros, Minas Gerais, CEP 39401-089, Brazil. ²⁰Fondo Patrimonio Natural para la Biodiversidad y Areas Protegidas, Calle 72 No. 12-65 piso 6, Bogotá, Colombia. ²¹Biological Dynamics of Forest Fragments Project, Environmental Dynamics Research Coordination, Instituto Nacional de Pesquisas da Amazonia, Manaus, Amazonas, CEP 69067-375, Brazil. ²²Centre for Crop Systems Analysis, Wageningen University, PO Box 430, 6700 AK Wageningen, The Netherlands. ²³Knowledge, Technology and Innovation Group, Wageningen University, PO Box 8130, 6700 EW Wageningen, The Netherlands. ²⁴Coordenação de Tecnologia e Inovação, Instituto Nacional de Pesquisas da Amazônia, Avenida André Araújo, 2936 - Aleixo, 69060-001 Manaus, Brazil. ²⁵Department of Physical and Environmental Sciences, Colorado Mesa University, 1100 North Avenue, Grand Junction, Colorado 81501, USA. ²⁶Department of Environmental Studies, Purchase College (State University of New York), Purchase, New York 10577, USA. ²⁷Instituto Boliviano de Investigación Forestal (IBIF), FCA-UAGRM, Casilla 6204, Santa Cruz de la Sierra, Bolivia. ²⁸World Agroforestry Centre (ICRAF), PO Box 30677 - 00100, Nairobi, Kenya. ²⁹Department of Geography, University of Wisconsin-Madison, 550 North Park Street, Madison, Wisconsin 53706, USA. ³⁰Departamento de Ecología y Recursos Naturales, Universidad Nacional Autónoma de México, México 04510 DF, México. ³¹Department of Ecology, Evolution and Environmental Biology, Columbia University, New York, New York 10027, USA. ³²Section of Ecoinformatics and Biodiversity, Department of Bioscience, Aarhus University, Aarhus 8000, Denmark. ³³Departamento de Ecología, Instituto de Biociências, Universidade de São Paulo, Rua do Matão, travessa 14, No. 321, São Paulo, CEP 05508-090, Brazil. ³⁴Universidade Federal do Sul da Bahia, Centro de Formação em Ciências Agroflorestais, Itabuna-BA, 45613-204, Brazil. ³⁵Department of Ecology, Evolution, & Behavior, University of Minnesota, Saint Paul, Minnesota 55108, USA. ³⁶Department of Plant Biology, University of Minnesota, Saint Paul, Minnesota 55108, USA. ³⁷School of Social Sciences, Geography Area, Universidad Pedagógica y Tecnológica de Colombia (UPTC), Tunja, Colombia. ³⁸Department of Geography, 4841 Ellison Hall, University of California, Santa Barbara, California 93106, USA. ³⁹Cr 5 No 14-05, PO Box 412, Cota, Cundinamarca, Colombia. ⁴⁰4007 18th St Northwest, Washington DC 20011, USA. ⁴¹Department of Biology, University of Maryland, College Park, Maryland 20742, USA. ⁴²Yale-NUS College, 12 College Avenue West, Singapore 138610. ⁴³Department of Biological Sciences, National University of Singapore, 14 Science Drive 4, Singapore 117574. ⁴⁴Departamento de Agricultura, Sociedad y Ambiente, El Colegio de la Frontera Sur - Unidad Villahermosa, 86280 Centro, Tabasco, México. ⁴⁵Institute for Biodiversity and Ecosystem Dynamics (IBED), University of Amsterdam, PO Box 94248, 1090 GE Amsterdam, The Netherlands. ⁴⁶Bonhoeffer College, Bruggertstraat 60, 7545 AX Enschede, The Netherlands. ⁴⁷Museu Paraense Emílio Goeldi, CP 399, CEP 66040-170, Belém, Brazil. ⁴⁸Department of Biological Sciences, Louisiana State University, Baton Rouge, Louisiana 70803-1705, USA. ⁴⁹Department of Biology, University of Regina, 3737 Wascana Parkway, Regina, Saskatchewan S4S 0A2, Canada.

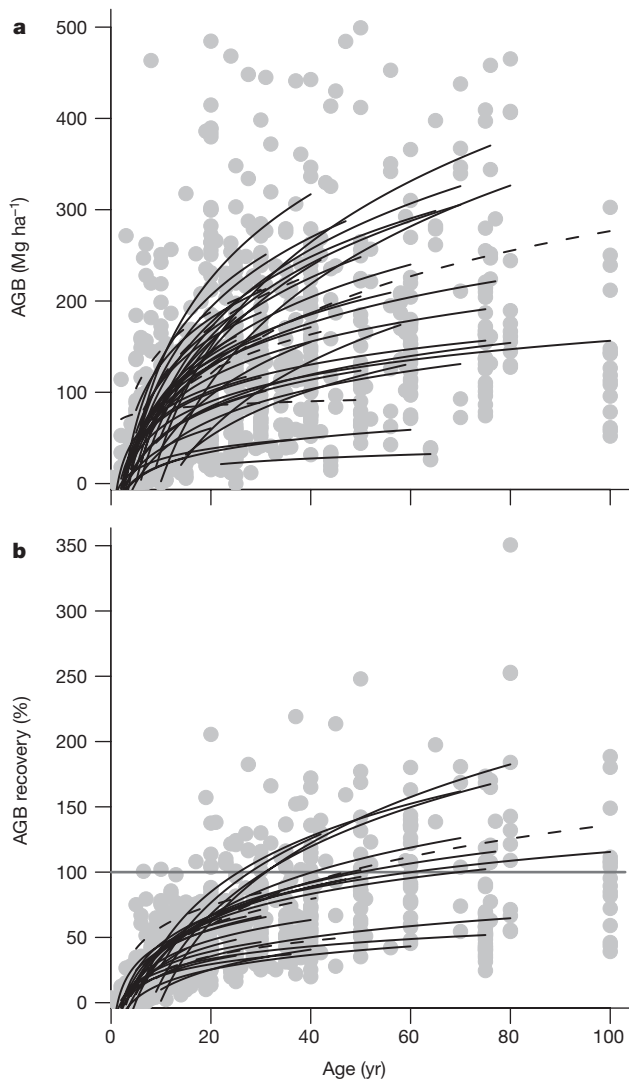


Figure 1 | Relationship between forest biomass and stand age using chronosequence studies in Neotropical secondary forest sites.

a, AGB ($N = 44$); **b**, AGB recovery ($N = 28$). Each line represents a different chronosequence. The original plots on which the regression lines are based are indicated in grey ($N = 1,364$ for AGB, $N = 995$ for AGB recovery). AGB recovery is defined as the AGB of the secondary forest plot compared with the median AGB of old-growth forest plots in the area, multiplied by 100. Significant relations (two-sided $P \leq 0.05$) are indicated by continuous lines; non-significant relationships (two-sided $P > 0.05$) are indicated by broken lines. Plots of 100 years old are also second-growth. See Extended Data Fig. 4 for the same figure with plots colour-coded by forest type.

or biased^{3,8,9} and we urgently need better-founded biomass recovery rates and resilience estimates.

Secondary forests deliver a suite of ecosystem services that are closely linked to the biomass resilience of these forests¹⁰. We define biomass resilience as the ability to (1) recover quickly after disturbance (that is, the absolute recovery) and (2) return to its original (pre-deforestation) state (that is, the relative recovery). Few studies have quantified forest recovery directly by monitoring secondary forest plots over time, and they typically cover only a few years (but see ref. 11). Chronosequence studies have evaluated different plots at different times after abandonment¹² and shown that recovery rates vary dramatically with climate¹³, soils¹⁴, and management intensity¹⁵. However, the meta-analyses so far^{13,16–18} did not consider Neotropical-wide environmental gradients and were not based on original data, making direct comparisons impossible because of variation in methodology and allometric biomass equations used.

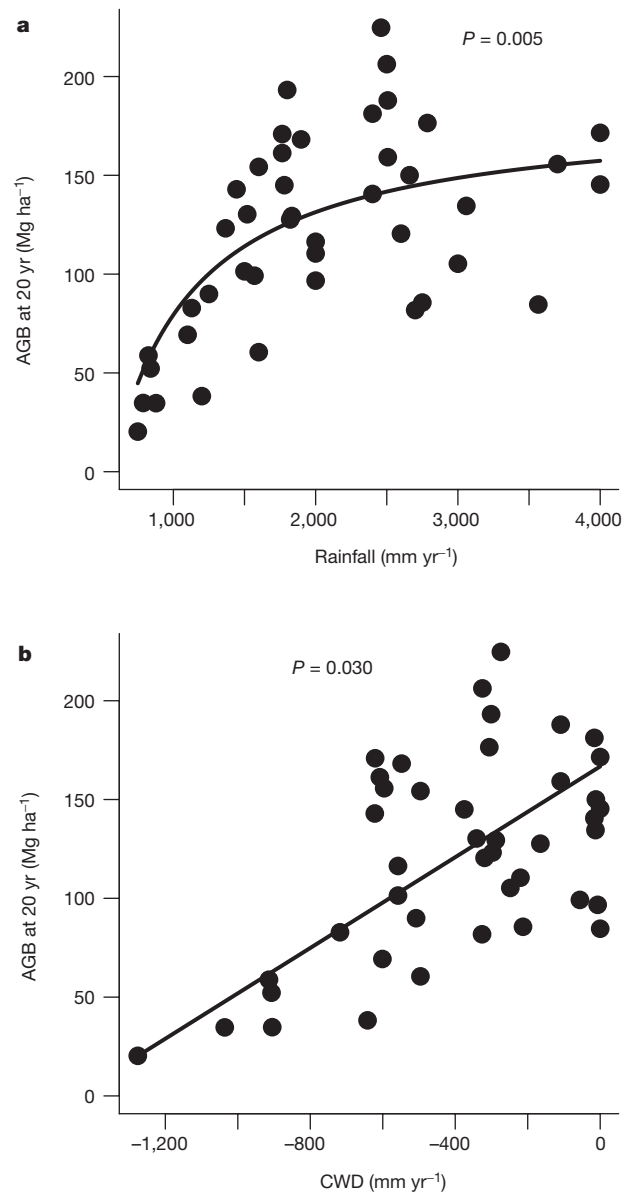


Figure 2 | AGB after 20 years. a, In relation to annual rainfall; **b**, in relation to CWD for Neotropical forest sites. Lines indicate predicted AGB at 20 years based on a multiple regression including $1/\text{rainfall}$, CWD, and rainfall seasonality ($R^2 = 0.59$). Other variables were kept constant at the mean across sites (two-sided $P < 0.005$ for $1/\text{rainfall}$; $P = 0.03$ for CWD). The third, less significant factor (rainfall seasonality) is shown in Extended Data Fig. 2. $N = 43$ sites (one site was excluded because no climatic data were available).

Here we quantify rates of recovery of aboveground biomass (AGB) stocks in secondary forests, and assess to what extent recovery rates are driven by abiotic site conditions, landscape forest cover, and previous land use. We hypothesize that recovery rates increase with resource availability (high rainfall¹³ and fertile soils) and decrease with degree of forest loss in the surrounding landscape matrix (implying lower seed availability), as well as with intensity of prior land use. We test these hypotheses using an unprecedented multi-site analysis including 45 sites, 1,468 plots, and >168,000 stems, spanning the major environmental and latitudinal gradients in the Neotropics, and we present a biomass recovery map to support policy decisions for the Neotropics.

We compiled data from 45 chronosequence studies (Extended Data Table 1); we also included old-growth plots for 28 sites with no signs of recent human disturbance. In each plot all stems ≥ 5 cm diameter

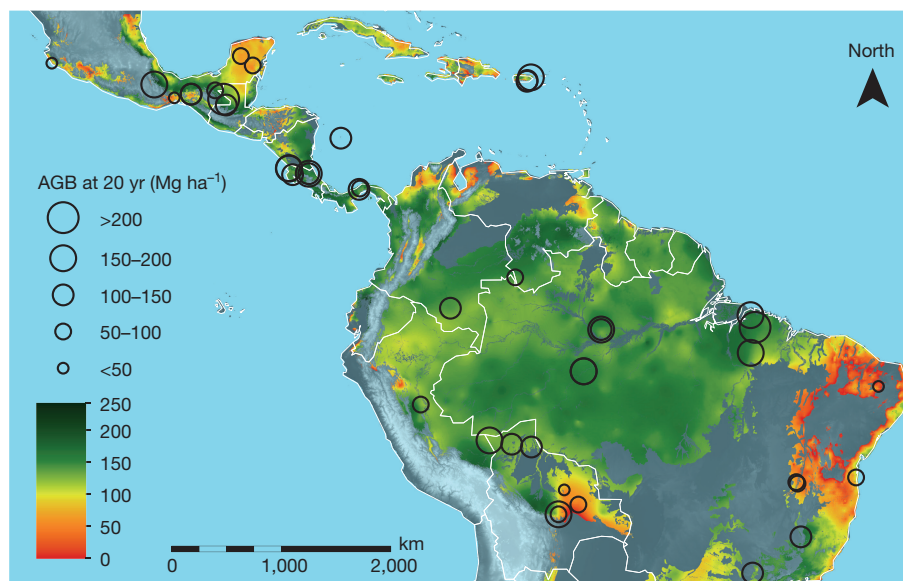


Figure 3 | Potential biomass recovery map of Neotropical secondary forests. The total potential AGB accumulation over 20 years of lowland secondary forest growth was calculated on the basis of a regression equation relating AGB with annual rainfall ($AGB = 135.17 - 103,950 \times 1/rainfall + 1.522 \times rainfall\ seasonality + 0.1148 \times CWD$; see Methods). The colour indicates the amount of forest cover recovery (red is low

recovery; green is high recovery). The 44 study sites are indicated by circles (the symbol on the ocean belongs to an island) and the size of the symbols scales with the AGB attained after 20 years. The grey areas do not belong to the tropical forest biome. The map focuses on lowland tropical forest (altitude <1,000 m). See Extended Data Fig. 5 for a colour-blind-friendly map.

were measured and identified, their biomass estimated using allometric equations, and summed across all trees to obtain live plot AGB.

For each site, AGB was modelled as a function of time elapsed since abandonment: that is, since the main human activity (crop production, cattle ranching) ceased at the site. Biomass resilience was quantified in two ways. For absolute recovery rate, the site-specific models ($N = 44$; one outlier excluded) were used to predict AGB at 20 years, a representative age for secondary forests in the Neotropics. For relative recovery, AGB was expressed as a percentage of the median AGB of old-growth forest plots in the area. AGB recovery was related to climatic water availability, soil cation exchange capacity (CEC), forest cover, and prior land use using multiple regression analysis. The best-supported equation was used to produce a biomass recovery map of the Neotropics.

Recovery of AGB showed a saturating relationship with stand age for the individual sites. After 20 years of secondary succession, AGB accumulation varied 11.3-fold (from 20 to 225 $Mg\ ha^{-1}$, average 121.8 ± 7.5 s.e.m.) across sites (Fig. 1a). Biomass recovery after 20 years, relative to old-growth forest AGB at the same site, varied from 25 to 85% across sites (Extended Data Fig. 1). Across sites, AGB after 20 years increased with annual precipitation ($P < 0.001$), climatic water deficit (CWD; $P < 0.001$, a higher value here means a lower deficit), and rainfall seasonality ($R^2 = 0.59$, $P < 0.0001$; Fig. 2, Extended Data Fig. 2a and Extended Data Table 2). There was considerable variation at a given level of water availability, which is also reflected in the root mean squared error of 31.7 $Mg\ ha^{-1}$. CEC, forest cover, and prior land use were not significant predictors of AGB accumulation across sites (Extended Data Fig. 2). For relative recovery, not only rainfall ($P = 0.040$) but also CEC ($P = 0.027$) had a significant positive effect on biomass recovery (Extended Data Table 2 and Fig. 1). The biomass recovery map (Fig. 3, see Extended Data Fig. 3 for an uncertainty map) shows high variation in potential AGB accumulation rates across the Neotropics, with low rates in dry forests in Mexico and high rates in humid forests in southern Mexico, Costa Rica, and large parts of the Amazon.

We show that AGB of 20-year-old secondary forest varies more than 11-fold across sites, with potentially large consequences for the carbon storage and mitigation potential of tropical forests (Supplementary Information S1). The carbon sequestration and mitigation potential of secondary forests is immense. Average biomass after 20 years

corresponds to an annual net carbon uptake of $3.05\ Mg\ C\ ha^{-1}\ yr^{-1}$, 11 times the uptake rates of Amazonian old-growth forests in 2010 ($0.28\ Mg\ C\ ha^{-1}\ yr^{-1}$ (ref. 19)) and 2.3 times the uptake rates of selectively logged Amazonian forests ($1.33\ Mg\ C\ ha^{-1}\ yr^{-1}$ (ref. 20)) where reduced impact logging techniques have been applied. Clearly, anthropogenic disturbances open up the canopy, enhance light availability, and set the system back to an earlier successional stage, leading to lower standing biomass but faster growth rates of the remaining forest stand. Although second-growth forests have substantially lower carbon stocks and biodiversity than the old-growth forests they replace, their carbon sequestering potential is high. Therefore, we urge halting deforestation and advocate actions that promote natural regeneration in deforested areas. Recognition of the significant carbon mitigation potential and other important services and values delivered by second-growth forests²¹ can be an important motivating factor to reach national targets for forest restoration inspired by the Convention on Biological Diversity Aichi Targets, the Bonn Challenge, and the New York Declaration on Forests.

Secondary forests differ dramatically in their biomass resilience, driven mainly by variation in water availability (Fig. 2, cf. ref. 13), although other factors play a role as well. Both higher rainfall and lower CWD increase plant water availability and extend the growing season, thereby increasing biomass growth of trees and forest stands²². Climate change scenarios predict less and/or more variable rainfall for several regions in the tropics²³, which may potentially hamper biomass recovery and forest resilience in these regions.

Soil fertility (CEC) had a significant positive effect on relative biomass recovery, but no effect on absolute recovery. Perhaps the effect of CEC was weak because for many sites CEC was obtained from a global database rather than measured *in situ*, because large differences in macroclimate may overrule more subtle differences in soil fertility, or because forest productivity is often limited by phosphorus²⁴ or nitrogen²⁵, which we did not measure. Forest cover in the surrounding matrix and prior land use did not affect biomass recovery (Extended Data Figs 1 and 2), perhaps because these were estimated. Forest recovery rate may slow down in isolated secondary forest patches because of reduced plant colonization and survival, harsher environmental conditions, and frequent disturbances. Biomass recovery did not differ between abandoned pastures and agricultural fields, possibly because

of high within-category variation in land-use intensity (such as use of fire and time under land use and frequency of cultivation cycles), which may strongly affect forest recovery^{15–17}.

Dry and moist forests differ substantially in old-growth forest biomass, and relative recovery may therefore be a better indicator of forest resilience than absolute recovery rates. It takes a median time of 66 years to recover to 90% of old-growth values. However, several mid-successional sites of 40–100 years old attained higher biomass than old-growth forest (Fig. 1b), which has also been found by modelling studies²⁶. This is most probably because of a high abundance of old trees of long-lived pioneer species in mid-successional sites, which tend to be large and store large amounts of carbon²⁷ before they die.

Several studies suggest that, once a certain threshold of disturbance is reached, tropical forests may collapse⁶ or switch to an alternative stable state⁷. Our study shows that forests can be resilient, and that their biomass resilience strongly depends on water availability. By mapping potential for biomass recovery across the Neotropics, attention can be focused on particular areas that should be conserved or treated with extra caution because they are more difficult to restore (slow recovery). The recovery map can also be used to identify areas with high carbon sequestration potential for United Nations collaborative initiative on Reducing Emissions from Deforestation and forest Degradation (REDD+) programmes, or where (assisted) natural regeneration, or restoration and afforestation activities, may have the highest chance of success^{28,29} (high recovery). Such a spatially explicit, resource-based approach paves the road towards a more sustainable design and management of human-modified tropical landscapes.

Online Content Methods, along with any additional Extended Data display items and Source Data, are available in the online version of the paper; references unique to these sections appear only in the online paper.

Received 7 May; accepted 2 December 2015.

Published online 3 February 2016.

- Hansen, M. C. *et al.* High-resolution global maps of 21st-century forest cover change. *Science* **342**, 850–853 (2013).
- IPCC. *2006 IPCC Guidelines for National Greenhouse Gas Inventories* (Institute for Global Environmental Strategies, 2006).
- Grace, J., Mitchard, E. & Gloor, E. Perturbations in the carbon budget of the tropics. *Glob. Change Biol.* **20**, 3238–3255 (2014).
- Chazdon, R. L. *Second Growth: The Promise of Tropical Forest Regeneration in an Age of Deforestation* Ch. 11 (Univ. Chicago Press, 2014).
- Food and Agriculture Organization of the United Nations. *Global Forest Resources Assessment*. FAO Forestry Paper 163 (FAO, 2010).
- Banks-Leite, C. *et al.* Using ecological thresholds to evaluate the costs and benefits of set-asides in a biodiversity hotspot. *Science* **345**, 1041–1045 (2014).
- Hirota, M., Holmgren, M., Van Nes, E. H. & Scheffer, M. Global resilience of tropical forest and savanna to critical transitions. *Science* **334**, 232–235 (2011).
- Pan, Y. *et al.* A large and persistent carbon sink in the world's forests. *Science* **333**, 988–993 (2011).
- Saatchi, S. S. *et al.* Benchmark map of forest carbon stocks in tropical regions across three continents. *Proc. Natl Acad. Sci. USA* **108**, 9899–9904 (2011).
- Lohbeck, M., Poorter, L., Martínez-Ramos, M. & Bongers, F. Biomass is the main driver of changes in ecosystem process rates during tropical forest succession. *Ecology* **96**, 1242–1252 (2015).
- Rozendaal, D. M. A. & Chazdon, R. L. Demographic drivers of tree biomass change during secondary succession in northeastern Costa Rica. *Ecol. Appl.* **25**, 506–516 (2015).
- Chazdon, R. L. *et al.* Rates of change in tree communities of secondary Neotropical forests following major disturbances. *Phil. Trans. R. Soc. B* **362**, 273–289 (2007).
- Becknell, J. M., Kucek, L. K. & Powers, J. S. Aboveground biomass in mature and secondary seasonally dry tropical forests: a literature review and global synthesis. *For. Ecol. Mgmt* **276**, 88–95 (2012).
- Becknell, J. M. & Powers, J. S. Stand age and soils as drivers of plant functional traits and aboveground biomass in secondary tropical dry forest. *Can. J. Forest Res.* **44**, 604–613 (2014).
- Jakovac, C. C., Peña-Claros, M., Kuyper, T. W. & Bongers, F. Loss of secondary-forest resilience by land-use intensification in the Amazon. *J. Ecol.* **103**, 67–77 (2015).

- Zarin, D. J. *et al.* Legacy of fire slows carbon accumulation in Amazonian forest regrowth. *Front. Ecol. Environ.* **3**, 365–369 (2005).
- Marín-Spiotta, E., Cusack, D. F., Ostertag, R. & Silver, W. L. in *Post-Agricultural Succession in the Neotropics* (ed. Myster, R. W.) 22–72 (Springer, 2008).
- Martin, P. A., Newton, A. C. & Bullock, J. M. Carbon pools recover more quickly than plant biodiversity in tropical secondary forests. *Proc. R. Soc. B* **280**, <http://dx.doi.org/10.1098/rspb.2013.2236> (2013).
- Brienen, R. J. W. *et al.* Long-term decline of the Amazon carbon sink. *Nature* **519**, 344–348 (2015).
- Rutishauser, E. *et al.* Rapid tree carbon stock recovery in managed Amazonian forests. *Curr. Biol.* **25**, R787–R788 (2015).
- Bongers, F., Chazdon, R., Poorter, L. & Peña-Claros, M. The potential of secondary forests. *Science* **348**, 642–643 (2015).
- Toledo, M. *et al.* Climate is a stronger driver of tree and forest growth rates than soil and disturbance. *J. Ecol.* **99**, 254–264 (2011).
- IPCC. *Climate Change 2014: Synthesis Report. Contribution of Working Groups I, II and III to the Fifth Assessment Report of the Intergovernmental Panel on Climate Change* (IPCC, 2014).
- Quesada, C. A. *et al.* Basin-wide variations in Amazon forest structure and function are mediated by both soils and climate. *Biogeosciences* **9**, 2203–2246 (2012).
- Davidson, E. A. *et al.* Recuperation of nitrogen cycling in Amazonian forests following agricultural abandonment. *Nature* **447**, 995–998 (2007).
- Fischer, R., Armstrong, A., Shugart, H. H. & Huth, A. Simulating the impacts of reduced rainfall on carbon stocks and net ecosystem exchange in a tropical forest. *Environ. Model. Softw.* **52**, 200–206 (2014).
- Mascaro, J., Asner, G. P., Dent, D. H., DeWalt, S. J. & Denslow, J. S. Scale-dependence of aboveground carbon accumulation in secondary forests of Panama: a test of the intermediate peak hypothesis. *For. Ecol. Mgmt* **276**, 62–70 (2012).
- Chazdon, R. L. Beyond deforestation: restoring forests and ecosystem services on degraded lands. *Science* **320**, 1458–1460 (2008).
- Birch, J. C. *et al.* Cost-effectiveness of dryland forest restoration evaluated by spatial analysis of ecosystem services. *Proc. Natl Acad. Sci. USA* **107**, 21925–21930 (2010).

Supplementary Information is available in the online version of the paper.

Acknowledgements This paper is a product of the 2ndFOR collaborative research network on secondary forests. We thank the owners of the secondary forest sites for access to their forests, all the people who have established and measured the plots, and the institutions and funding agencies that supported them. We thank J. Zimmerman for the use of plot data, and the following agencies for financial support: Australian Department of Foreign Affairs and Trade-DFAT, CGIAR-FTA, CIFOR, Colciencias grant 1243-13-16640, Consejo Nacional de Ciencia y Tecnología (SEP-CONACYT 2009-129740 for ReSerBos, CONACYT 33851-B), Conselho Nacional de Desenvolvimento Científico e Tecnológico (CNPq: 563304/2010-3, 562955/2010-0, 574008/2008-0 and PQ 307422/2012-7), FOMIX-Yucatan (YUC-2008-C06-108863), ForestGEO, Fundação de Amparo à Pesquisa de Minas Gerais (FAPEMIG CRA APQ-00001-11), Fundación Ecológica de Cuixmala, Heising-Simons Foundation, HSB, ICETEX, Instituto Internacional de Educação do Brasil-IEB, Instituto Nacional de Serviços Ambientais da Amazônia -Servamb-INPA, Inter-American Institute for Global Change (Tropi-Dr Network CRN3-025) via a grant from the US National Science Foundation (grant GEO-1128040), Motta Family Foundation, NASA Terrestrial Ecology Program, National Science Foundation (NSF-CNH-RCN grant 1313788 for Tropical Reforestation Network: Building a Socioecological Understanding of Tropical Reforestation (PARTNERS), NSF DEB-0129104, NSF BCS-1349952, NSF Career Grant DEB-1053237, NSF DEB 1050957, 0639393, 1147429, 0639114, and 1147434), NUFFIC, USAID (BOLF0R), Science without Borders Program (CAPES/CNPq) grant number 88881.064976/2014-01, The São Paulo Research Foundation (FAPESP) grant 2011/06782-5 and 2014/14503-7, Silicon Valley Foundation, Stichting Het Kronendak, Tropenbos Foundation, University of Connecticut Research Foundation, Wageningen University (INREF Terra Preta programme and FOREFRONT programme). This is publication number 683 in the Technical Series of the Biological Dynamics of Forest Fragments Project BDFFP-INPA-SI. This study was partly funded by the European Union's Seventh Framework Programme (FP7/2007-2013) under grant agreement number 283093; Role Of Biodiversity In climate change mitigation (ROBIN).

Author Contributions L.P., F.B. and D.R. conceived the idea and coordinated the data compilations, D.R. analysed the data, L.P., F.B., E.N.B. and R.C. contributed to analytical tools used in the analysis, E.N.B. and A.M.A.Z. made the map, L.P. wrote the paper, and all co-authors collected field data, discussed the results, gave suggestions for further analyses and commented on the manuscript.

Author Information Plot-level AGB data of 41 sites are available from the Dryad Digital Repository: <http://dx.doi.org/10.5061/dryad.82vr4>, and for four sites they can be requested from L.P. Reprints and permissions information is available at www.nature.com/reprints. The authors declare no competing financial interests. Readers are welcome to comment on the online version of the paper. Correspondence and requests for materials should be addressed to L.P. (lourens.poorter@wur.nl).

METHODS

Site description. We compiled the largest data set of chronosequence studies in the lowland Neotropics so far, including 1,468 plots established in 45 forest sites (Extended Data Table 1), containing 168,210 tree stems. The sites were located in eight countries, covering the full latitudinal range in the tropics varying from 20°N in Mexico to 22°S in Brazil. We focused on lowland sites, generally below 1,000 m altitude. Annual rainfall varied fivefold across sites (from 750 to 4,000 mm yr⁻¹), thus all major lowland forest types were included. Soil CEC varied 33-fold across sites (from 2 to 65 cmol(+) kg⁻¹). Forest cover in the landscape ranged from 31 to 100% across sites.

Site conditions. We assessed whether biomass recovery rates were related to abiotic site conditions (rainfall, soil fertility), and land-use intensity (prior land use and percentage forest cover in the surrounding matrix). For each site, mean annual rainfall was obtained from the nearest climatological station. Biomass recovery should ultimately respond to plant water availability, which is a function of annual rainfall and its seasonal distribution, topography, soil depth, and the water holding capacity of the soil. Rainfall seasonality (expressed as a coefficient of variation of rainfall) was obtained from WorldClim³⁰ and CWD (in millimetres per year) from http://chave.ups-tlse.fr/pantropical_allometry.htm. CWD is the amount of water lost during dry months (defined as months where evapotranspiration exceeds rainfall), and is calculated as the total rainfall minus evapotranspiration during dry months. This number is by definition negative, and sites with CWD of 0 are not seasonally water stressed. CEC (in centimoles of positive charge per kilogram of soil) was used as an indicator of soil fertility of the site. Ideally, local soil data should be used, but these were only available for 12 sites. For the other sites, CEC data were obtained from the Harmonized World Soil Database (HWSD)³¹. For those 12 sites, the local CEC and HWSD data are indeed strongly positively correlated ($r=0.84$, $P<0.0006$, $n=12$), indicating that the HWSD ranks the sites well in terms of CEC. When local soil fertility data were available, the CEC of the old-growth forest was used, as this indicates potential site fertility, which is also included in the world soil database. The HWSD database did not contain data on soil nitrogen and phosphorus. Phosphorus is thought to limit plant growth in highly weathered and leached tropical soils and correlates well with the productivity of old-growth Amazonian forests²⁴. Nitrogen may be more limiting during the first decades of secondary succession because a large part of vegetation nitrogen is volatilized when the slashed vegetation is burned²⁵, while soil preparation, crop cultivation, and nutrient leaching may further deplete soil nutrients. Indeed, early successional forests have relatively many nitrogen-fixing trees. To describe the landscape matrix, we estimated per site, for all plots combined, the average cover in the following five land use classes in a 1 km radius around the plots: mature forest, secondary forest, plantations/agroforestry systems, agriculture/pasture, other. This estimate is based on the long-term field experience of the authors at the site where they worked. We then calculated per site the average percentage total forest cover (of mature and secondary forest) in a 1 km radius around the plots. We used total forest cover because forests improve microclimatic conditions at the landscape level and act as important sources of seeds and biotic agents (mammal and bird dispersal agents, mycorrhizae) that may help to speed up the rate of secondary succession. We classified the prior land use of each site as cattle ranching or shifting cultivation (or a combination of these two), which are the two major land-use types where forest regeneration occurs in the Neotropics. We acknowledge that different land use practices, such as fire frequency¹⁶ and length of cultivation¹⁵, could affect biomass recovery rates of abandoned fields, but it is very difficult to obtain that information in a consistent and quantitative way across all sites.

Plots. Plot size varied from 0.01 to 1 ha. Most plots were rectangular, with a length varying from 20 to 200 m and width ranging from 1 to 50 m. The mean plot area across all ~1,468 plots was 947 m², and the mean plot area across all 45 sites was 1,273 m². On average 33 (5–291) plots were established per chronosequence. Chronosequence sites varied in the range of stand ages across the included secondary forest plots (Extended Data Table 1). For 28 out of the 45 sites, old-growth plots were included. Old-growth forests did not have signs of recent human disturbance, and were at least 100 years old. In most cases, the sampling design was the same as for secondary forest plots; however, for five of the sites, old-growth plots were slightly larger, for one site smaller. In each plot, all woody trees, shrubs, and palms ≥ 5 cm stem diameter at breast height (at 1.3 m height) were measured for their diameter and identified to species, with the exception of three sites for which only data for trees ≥ 10 cm diameter at breast height were available.

Tree biomass. We first evaluated how estimates of live AGB varied on the basis of the application of three frequently used sets of allometric equations. We calculated live AGB for each tree using equations from refs 32–34 (Supplementary Information S2). The equations in ref. 32 are based on stem

diameter only, and the equations in refs 33, 34 are based on a combination of stem diameter and wood density. Palms were treated in the same way as trees³⁵, which may slightly overestimate palm biomass. Biomass was summed across all trees to obtain live plot AGB. The three different equations from refs 32–34 resulted in small differences in absolute plot AGB estimates for dry forests (average AGB after 20 years ranged from 68 to 85 Mg ha⁻¹ among the three equations), but yielded larger differences in AGB estimates for moist forest (precipitation 1,500–2,500 mm yr⁻¹, AGB after 20 years ranged from 142 to 179 Mg ha⁻¹; Extended Data Fig. 6). For 20-year-old forest, the earlier widely used equations^{32,33} predicted about 21–26% more biomass than the more recently developed equation (Extended Data Fig. 6). These differences become even greater with increasing forest age, with large consequences for assessing the magnitude of carbon uptake and storage in tropical forests (see, for example, ref. 19), as moist forests contribute most to the current forested area in the Neotropics. For further analyses we used the equation in ref. 34 because it provides an allometric equation based on the largest harvested tree data set analysed so far (and includes and extends the equation of ref. 33), including many secondary forest species for trees from wet and dry forests, for trees of most tropical continents. It is ecologically very relevant and methodologically elegant, as it uses a correction factor E . This bioclimatic stress variable takes temperature variability, precipitation variability, and drought intensity into account, and therefore continuous variation in site aridity. The equation in ref. 34 also takes variation in wood density into account, which is an important source of plot AGB variation across the Neotropics³⁶. For one site (Providencia Island) for which no E value was available, we estimated E from a regression equation relating E to annual rainfall.

Data about species-specific wood density (in grams per cubic centimetre) came from the local sites, or from the Neotropical data of a global wood density database^{37,38} (<http://datadryad.org/handle/10255/dryad.235>), henceforth referred to as 'Dryad'. For all estimates of wood density, we used the data source (local or Dryad) that had the highest level of taxonomic resolution. In the case of the same level of taxonomic resolution, we used the local data source. If no wood density information was available at the species level, then genus- or family-level wood density values were used, as wood density is phylogenetically strongly conserved³⁹. Across all sites except Surutu 1 and 2, Cayey, and Bolpebra, 94.0% of the trees of the secondary and old-growth plots had been identified to species (range 74.4–100%), 97.9% to genus (range 90.8–100%), and 98.9% to family (range 94.9–100%). For the other four sites, 36.0–55.6% of the trees had been identified to species, 61.6–86% to genus, and 61.6–86% to family.

Plot structure. Biomass was summed across all trees in a plot to obtain live plot AGB and expressed on a per hectare basis (AGB, in megagrams per hectare). For one site (San Carlos) the original tree inventory data were not available anymore, so for this site we used the plot biomass that the author had estimated using locally derived allometric equations. For plots with a nested design, we calculated AGB per hectare by extrapolating the biomass of trees in smaller size classes that were measured in a part of the plot only to the total area measured, thus assuming that forest structure within the plot did not vary. For four sites, only trees ≥ 10 cm diameter at breast height were inventoried, and for these sites a correction factor was used to obtain the estimated plot AGB when trees between 5 and 10 cm diameter at breast height would have been included. Plot AGB was therefore multiplied by 1.18 for dry forest and by 1.03 for moist forest (compare ref. 40). Some plots had extremely high AGB values (>500 Mg ha⁻¹), because of the occurrence of a single large tree, in combination with a small plot size. These outliers (2.5% of the total number of plots) were excluded from the analysis. One site (Marques de Comillas) had extremely high average AGB (>100 Mg ha⁻¹) 2 years after land abandonment, because of a combination of many large remnant forest trees being left during land use, and a small plot size. This site was excluded from the analysis. Our analysis focused on AGB only, which should be a good indicator of carbon recovery over time, as below-ground biomass in roots scales tightly with AGB of trees⁴¹, and soil organic matter (which includes necromass of dead fallen trees and roots) is rather constant with time after abandonment¹⁸.

Statistical analyses. No statistical methods were used to predetermine sample size. To evaluate how AGB (estimated with the equation from ref. 34) recovered over time, we modelled AGB in each site as a function of natural-logarithm-transformed age. We included an intercept, as in some cases there was AGB at time zero because remnant trees were left during forest clearance. Biomass resilience was quantified in two complementary ways: the absolute recovery rate and the relative recovery rate. For absolute recovery, the site-specific models ($N=44$ sites) were used to predict AGB at 10 and 20 years, as these ages were included in the age range of most sites, and are representative ages for secondary forests. To calculate annual carbon sequestration rates, we used the average AGB attained

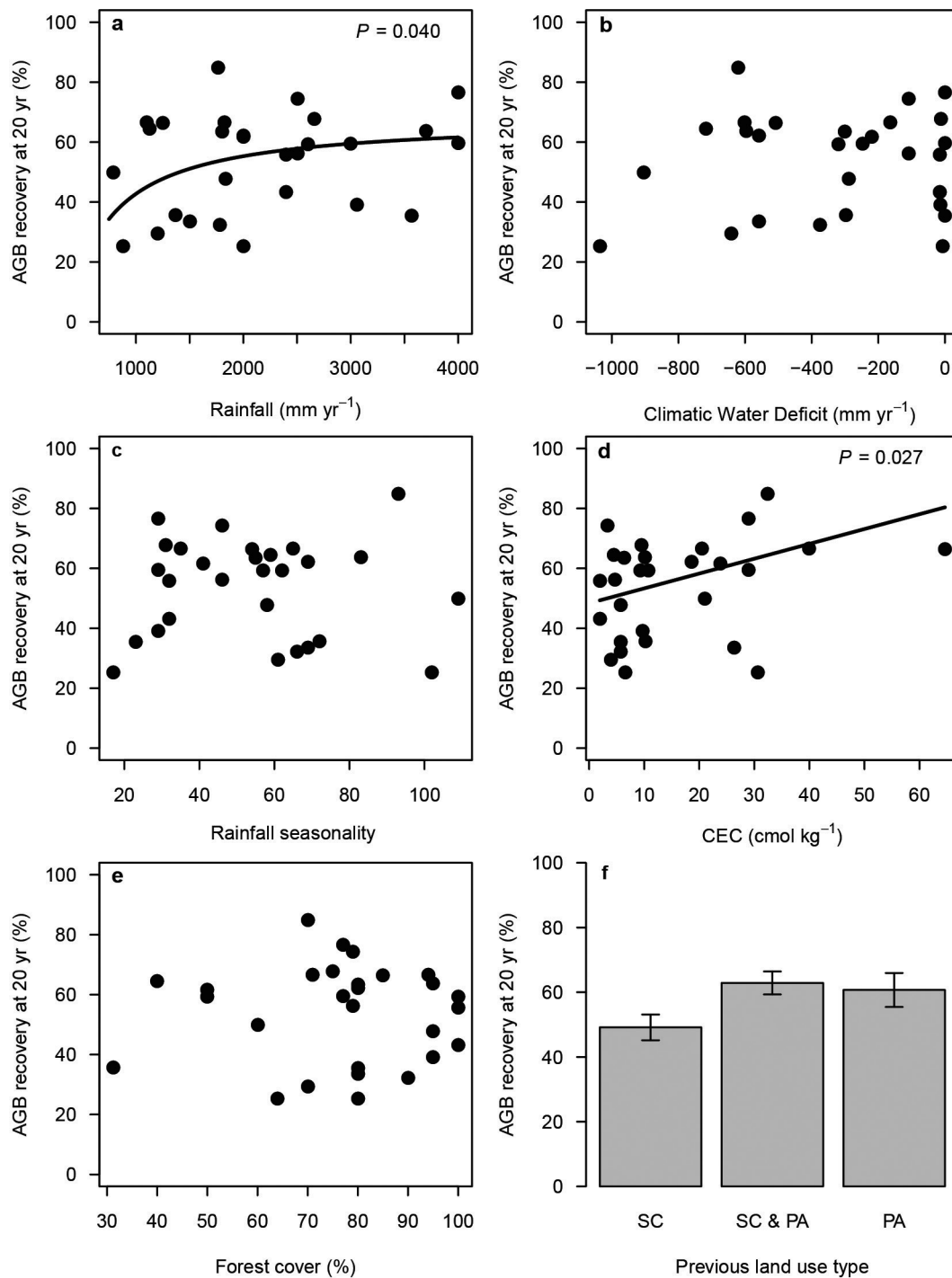
after 20 years, multiplied it by 0.5 (which is the average carbon value in dry biomass), and divided it by 20. To evaluate how fast AGB of secondary forests recovers towards old-growth forest values, we calculated the relative AGB recovery as the AGB of the secondary forest plot compared with the median AGB of old-growth forest plots in the area (as a percentage). For each site, we estimated the recovery time as the time needed to recover to 90% of old-growth values. We used time to recover to 90%, rather than to recover 100% of old-growth values, as it indicates when the biomass is close to old-growth values. To attain the full 100% may take much more time, as we modelled biomass build-up to show an asymptotic relationship with time. This study aimed to assess the rates of recovery of tree biomass under conditions where regeneration is occurring naturally. Sometimes, succession can be arrested owing to high-intensity land use or seed limitation. We did not target sites where succession was arrested, so it is possible that our 'average' conditions could have overestimated rates of recovery when considering all potential areas. However, neither did we specifically select sites that were regenerating particularly fast. Given the high number of sites and plots across the Neotropics that cover the entire range of typical land-use types and intensities, we are confident that we provide realistic rates of biomass accumulation for dominant land-use types and intensities in the Neotropics.

To evaluate how predicted absolute and relative recovery of AGB after 20 years varied with abiotic site conditions and land-use intensity, we used multiple regression analysis. We related AGB recovery to rainfall, rainfall seasonality, CWD, CEC, forest cover in the landscape matrix, and prior land use (pasture, mix of pasture and agriculture, agriculture) for 43 sites (for one island site no WorldClim data were available). AGB showed a saturating relationship with rainfall; therefore we used $1/\text{rainfall}$ as a predictor rather than absolute rainfall or the natural logarithm of rainfall, which improved model fits. We compared models of all possible combinations of predictors based on Akaike's information criterion adjusted for small sample sizes (AIC_c), and selected the best-supported model with the lowest AIC_c . All analyses were performed in R 3.1.2 (ref. 42).

On the basis of our regression analysis, we constructed a potential biomass recovery map of the Neotropics at a resolution of 1 km^2 . First, a map of world ecoregions was obtained from the Nature Conservancy (http://maps.tnc.org/gis_data.html; last accessed on 26 January 2015). Eight hundred and sixty-seven distinct units were categorized into 14 biomes in 8 biogeographical realms⁴³. Of these 14 biomes, three are relevant to our results: (1) tropical and subtropical moist broadleaf forests, (2) tropical and subtropical dry broadleaf forests, and (3) tropical and subtropical coniferous forests. Our scaled-up study region was then defined as the full spatial extent encompassing these three biomes in Central or South America, the region in which our network of study sites was located. Total annual precipitation was calculated by summing the individual monthly totals provided by WorldClim. Data for mean annual rainfall (defined as the average of 1950–2000) and rainfall seasonality (defined as variable 'BIO15' in WorldClim) was obtained at a 30 s resolution (approximately $1\text{ km} \times 1\text{ km}$) from WorldClim (<http://www.worldclim.org/current>), and CWD was obtained from http://chave.ups-tlse.fr/pantropical_allometry.htm. We then calculated the total potential AGB accumulation over 20 years of secondary forest growth (assuming that the initial year 0 condition was a fully cleared area), based on annual rainfall, rainfall seasonality, and CWD, because they were included in the best model explaining absolute recovery (Extended Data Table 2). The regression equation obtained in this study, relating AGB after 20 years with the climatic variables, was $\text{AGB at } 20\text{ yr} = 135.17 - 103,950 \times 1/\text{rainfall} + 1.521983 \times \text{rainfall seasonality} + 0.1148 \times \text{CWD}$. Estimated AGB would then indicate the absolute biomass recovery potential. We stress that this is a potential biomass recovery map based on the relationship between recovery and rainfall for our sites; realized local recovery may vary because of differences in local soil conditions, land use history, the surrounding matrix, and availability of seed sources. We also made an uncertainty map of potential biomass based on the confidence interval of the predicted mean AGB at 20 years obtained from the multiple regression. We calculated the confidence interval of the predicted AGB at 20 years for each pixel based on $1/\text{rainfall}$, CWD, and rainfall seasonality. The relative uncertainty for each pixel was calculated as $100 \times (0.5 \times 95\% \text{ confidence interval of the mean})/\text{predicted AGB}$. For the maps we focused on lowland forest (<1,000 m altitude), between the Tropics of Cancer and Capricorn. To make the maps, we had to extrapolate very little beyond our climatic parameter space; our sites cover a rainfall range from 750 to 4,000 mm yr^{-1} . Sites with rainfall >4,000 mm yr^{-1} (where we extrapolate with our equation) cover only 0.88% of the lowland Neotropics.

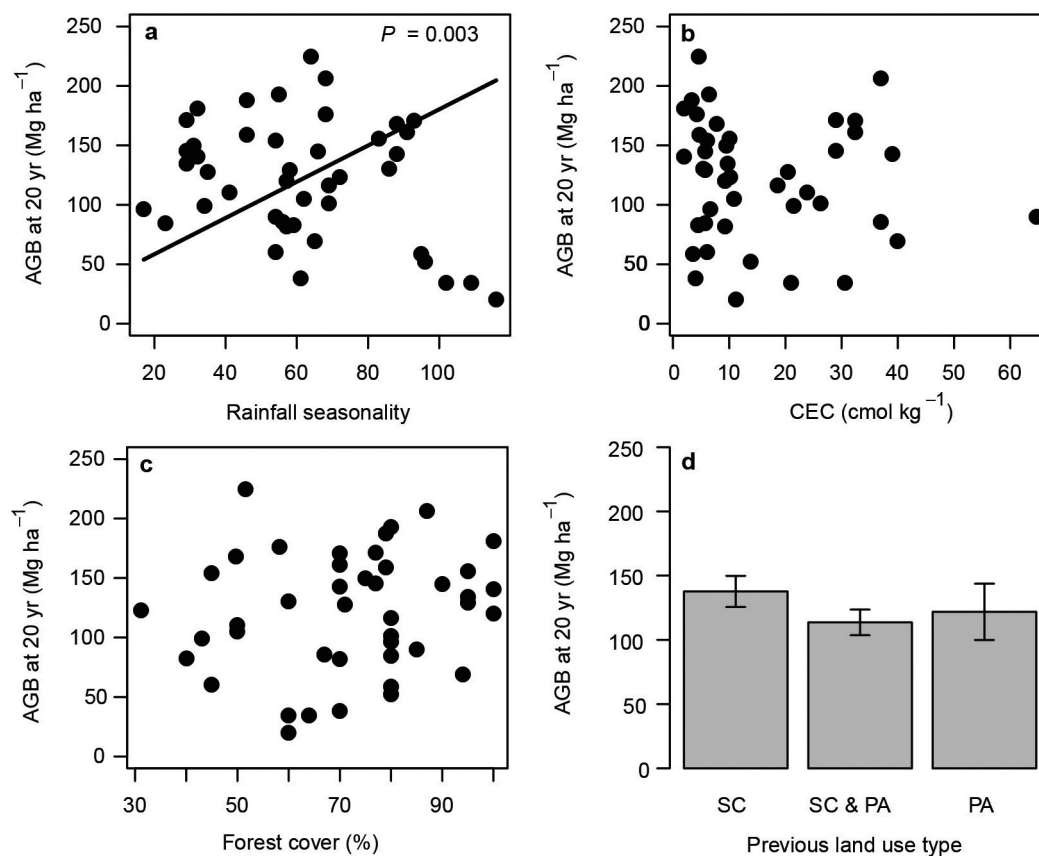
30. Hijmans, R. J., Cameron, S. E., Parra, J. L., Jones, P. G. & Jarvis, A. Very high resolution interpolated climate surfaces for global land areas. *Int. J. Climatol.* **25**, 1965–1978 (2005).
31. Nachtergaele, F., van Velthuizen, H., Verelst, L. & Wiberg, D. *Harmonized World Soil Database Version 1.2* (FAO and IIASA, 2012).
32. Pearson, R., Walker, S. & Brown, S. *Source Book for Land Use, Land-Use Change and Forestry Projects* (World Bank, 2005).
33. Chave, J. et al. Tree allometry and improved estimation of carbon stocks and balance in tropical forests. *Oecologia* **145**, 87–99 (2005).
34. Chave, J. et al. Improved allometric models to estimate the aboveground biomass of tropical trees. *Glob. Change Biol.* **20**, 3177–3190 (2014).
35. Clark, D. B. & Clark, D. A. Landscape-scale variation in forest structure and biomass in a tropical rain forest. *For. Ecol. Mgmt* **137**, 185–198 (2000).
36. Mitchard, E. T. A. et al. Markedly divergent estimates of Amazon forest carbon density from ground plots and satellites. *Glob. Ecol. Biogeogr.* **23**, 935–946 (2014).
37. Chave, J. et al. Towards a worldwide wood economics spectrum. *Ecol. Lett.* **12**, 351–366 (2009).
38. Zanne, A. E. et al. Data from: Towards a worldwide wood economics spectrum. <http://dx.doi.org/10.5061/dryad.234> (Dryad Digital Repository, 2009).
39. Chave, J. et al. Regional and phylogenetic variation of wood density across 2456 Neotropical tree species. *Ecol. Appl.* **16**, 2356–2367 (2006).
40. Poorter, L. et al. Diversity enhances carbon storage in tropical forests. *Glob. Ecol. Biogeogr.* **24**, 1314–1328 (2015).
41. Poorter, H. et al. How does biomass distribution change with size and differ among species? An analysis for 1200 plant species from five continents. *New Phytol.* **208**, 736–749 (2015).
42. R Core Team. R: a language and environment for statistical computing (R Foundation for Statistical Computing, 2014).
43. Olson, D. M. et al. Terrestrial ecoregions of the world: a new map of life on Earth. *Bioscience* **51**, 933–938 (2001).
44. Broadbent, E. N. et al. Integrating stand and soil properties to understand foliar nutrient dynamics during forest succession following slash-and-burn agriculture in the Bolivian Amazon. *PLoS ONE* **9**, e86042 (2014).
45. Peña-Claros, M. Changes in forest structure and species composition during secondary forest succession in the Bolivian Amazon. *Biotropica* **35**, 450–461 (2003).
46. Toledo, M. & Salick, J. Secondary succession and indigenous management in semideciduous forest fallows of the Amazon basin. *Biotropica* **38**, 161–170 (2006).
47. Kennard, D. K. Secondary forest succession in a tropical dry forest: patterns of development across a 50-year chronosequence in lowland Bolivia. *J. Trop. Ecol.* **18**, 53–66 (2002).
48. Steininger, M. K. Secondary forest structure and biomass following short and extended land use in central and southern Amazonia. *J. Trop. Ecol.* **16**, 689–708 (2000).
49. Piotto, D. *Spatial Dynamics of Forest Recovery after Swidden Cultivation in the Atlantic Forest of Southern Bahia, Brazil*. PhD thesis, Yale Univ. (2011).
50. Vieira, I. C. G. et al. Classifying successional forests using Landsat spectral properties and ecological characteristics in eastern Amazonia. *Remote Sens. Environ.* **87**, 470–481 (2003).
51. Williamson, G. B., Bentos, T. V., Longworth, J. B. & Mesquita, R. C. G. Convergence and divergence in alternative successional pathways in Central Amazonia. *Plant Ecol. Divers.* **7**, 341–348 (2014).
52. Madeira, B. G. et al. Changes in tree and liana communities along a successional gradient in a tropical dry forest in south-eastern Brazil. *Plant Ecol.* **201**, 291–304 (2009).
53. Cabral, G. A. L., Sampaio, E. V. S. B. & de Almeida-Cortez, J. S. Estrutura espacial e biomassa da parte aérea em diferentes estádios successionalis de caatinga, em Santa Teresinha, Paraíba. *Rev. Bras. Geogr. Fis.* **6**, 566–574 (2013).
54. Junqueira, A. B., Shepard, G. H. & Clement, C. R. Secondary forests on anthropogenic soils conserve agrobiodiversity. *Biodivers. Conserv.* **19**, 1933–1961 (2010).
55. Vester, F. M. & Cleef, A. M. Tree architecture and secondary tropical rain forest development - a case study in Araracuara, Colombian Amazonia. *Flora* **193**, 75–97 (1998).
56. Ruiz, J., Fandino, M. C. & Chazdon, R. L. Vegetation structure, composition, and species richness across a 56-year chronosequence of dry tropical forest on Providencia Island, Colombia. *Biotropica* **37**, 520–530 (2005).
57. Saldarriaga, J. G., West, D. C., Tharp, M. L. & Uhl, C. Long-term chronosequence of forest succession in the upper Rio Negro of Colombia and Venezuela. *J. Ecol.* **76**, 938–958 (1988).
58. Powers, J. S., Becknell, J. M., Irving, J. & Perez-Aviles, D. Diversity and structure of regenerating tropical dry forests in Costa Rica: geographic patterns and environmental drivers. *For. Ecol. Mgmt* **258**, 959–970 (2009).
59. Chazdon, R. L., Brenes, A. R. & Alvarado, B. V. Effects of climate and stand age on annual tree dynamics in tropical second-growth rain forests. *Ecology* **86**, 1808–1815 (2005).
60. Letcher, S. G. & Chazdon, R. L. Rapid recovery of biomass, species richness, and species composition in a forest chronosequence in northeastern Costa Rica. *Biotropica* **41**, 608–617 (2009).
61. van Breugel, M., Martínez-Ramos, M. & Bongers, F. Community dynamics during early secondary succession in Mexican tropical rain forests. *J. Trop. Ecol.* **22**, 663–674 (2006).

62. Mora, F. *et al.* Testing chronosequences through dynamic approaches: time and site effects on tropical dry forest succession. *Biotropica* **47**, 38–48 (2015).
63. Orihuela-Belmonte, D. E. *et al.* Carbon stocks and accumulation rates in tropical secondary forests at the scale of community, landscape and forest type. *Agric. Ecosyst. Environ.* **171**, 72–84 (2013).
64. Lebrija-Trejos, E., Bongers, F., Pérez-García, E. A. & Meave, J. A. Successional change and resilience of a very dry tropical deciduous forest following shifting agriculture. *Biotropica* **40**, 422–431 (2008).
65. Dupuy, J. M. *et al.* Patterns and correlates of tropical dry forest structure and composition in a highly replicated chronosequence in Yucatan, Mexico. *Biotropica* **44**, 151–162 (2012).
66. van Breugel, M. *et al.* Succession of ephemeral secondary forests and their limited role for the conservation of floristic diversity in a human-modified tropical landscape. *PLoS ONE* **8**, e82433 (2013).
67. Denslow, J. S. & Guzman, S. Variation in stand structure, light and seedling abundance across a tropical moist forest chronosequence, Panama. *J. Veg. Sci.* **11**, 201–212 (2000).
68. Marín-Spiotta, E., Ostertag, R. & Silver, W. L. Long-term patterns in tropical reforestation: plant community composition and aboveground biomass accumulation. *Ecol. Appl.* **17**, 828–839 (2007).
69. Aide, T. M., Zimmerman, J. K., Pascarella, J. B., Rivera, L. & Marciano-Vega, H. Forest regeneration in a chronosequence of tropical abandoned pastures: implications for restoration ecology. *Restor. Ecol.* **8**, 328–338 (2000).



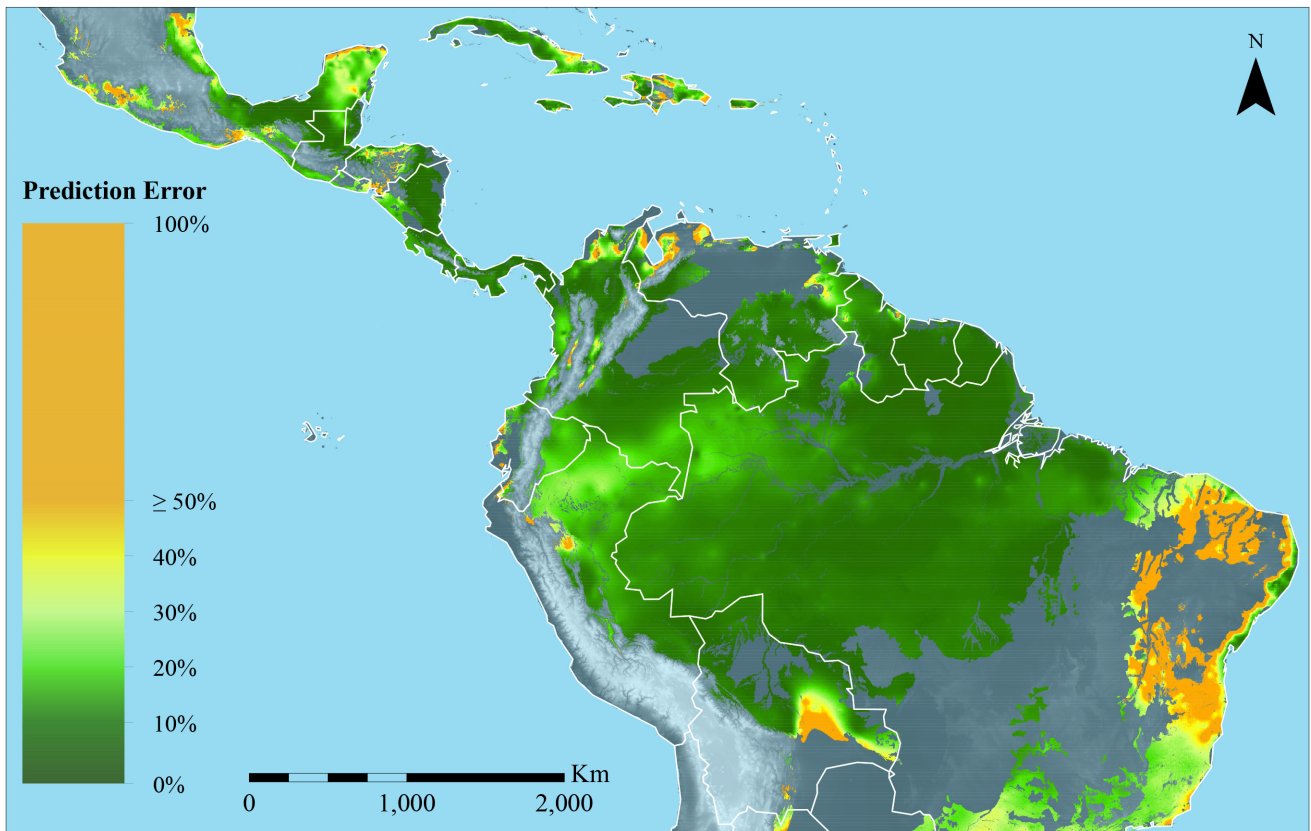
Extended Data Figure 1 | Relative recovery of AGB after 20 years in relation to abiotic factors, forest cover, and land use. a, Annual precipitation; b, CWD; c, rainfall seasonality; d, CEC; e, percentage forest cover in the surrounding matrix; f, previous land use (SC, shifting cultivation, $N = 17$; SC & PA, some plots shifting cultivation, some plots

pasture, $N = 2$; PA, pasture, $N = 9$; means \pm s.e.m. are shown). Relative recovery is expressed as the ratio of AGB after 20 years over median AGB of old-growth forest (as a percentage). Regression lines are shown while keeping the other variable constant at the mean value across sites ($P = 0.040$ for $1/\text{rainfall}$, $P = 0.027$ for CEC, $R^2 = 0.23$, $N = 28$ Neotropical forest sites).



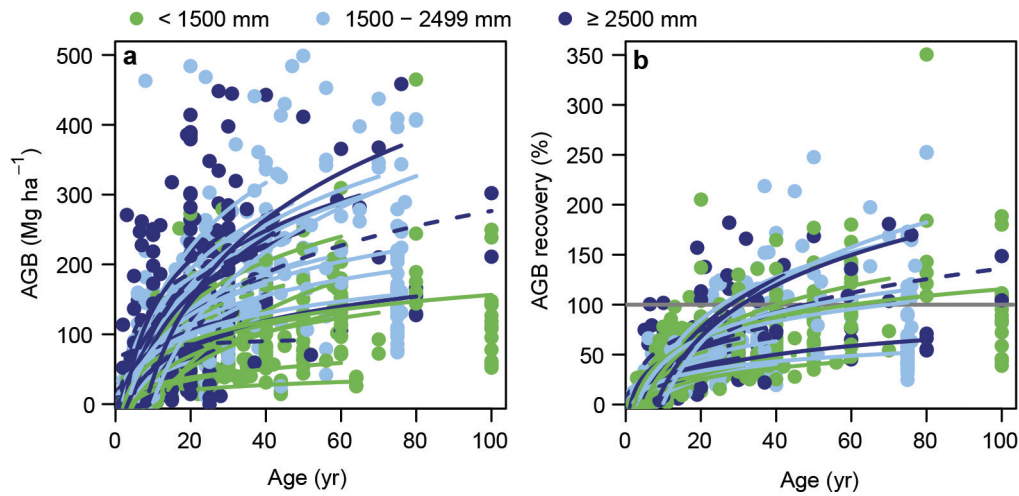
Extended Data Figure 2 | AGB recovery after 20 years in relation to abiotic factors, forest cover, and land use. a, Rainfall seasonality; b, CEC; c, percentage forest cover in the surrounding matrix; d, previous land use (SC, $N = 19$; SC & PA, $N = 9$; PA, $N = 15$; means \pm s.e.m. are shown).

For rainfall seasonality, the regression line is shown based upon the multiple regression model that also includes rainfall and CWD, and where these variables were kept constant at the mean value across sites (two-sided $P = 0.003$, see Fig. 2 for these models for rainfall and CWD).



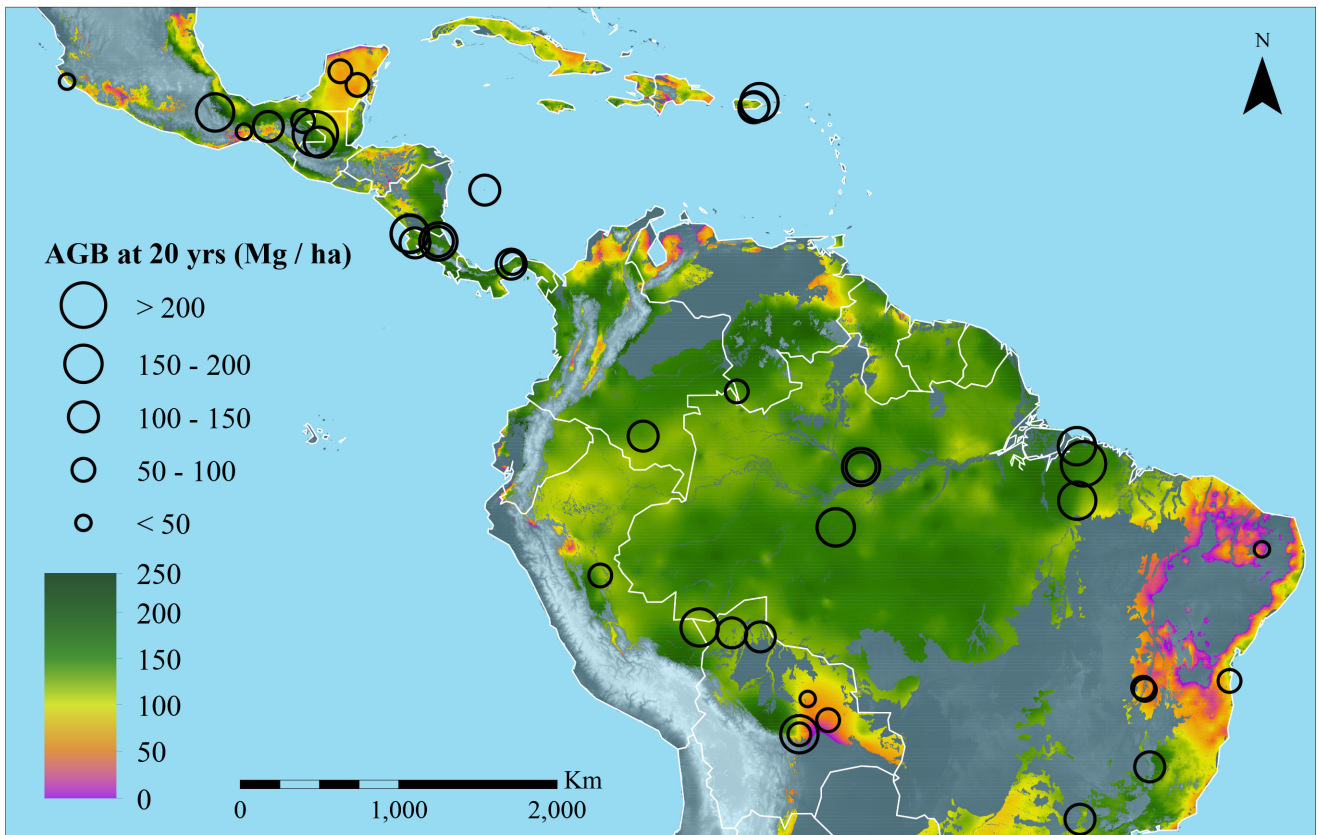
Extended Data Figure 3 | Uncertainty map of potential biomass recovery of Neotropical secondary forests. The uncertainty is based on the 95% confidence interval of the mean predicted AGB after 20 years (see Fig. 3 and Methods). It is expressed as a percentage of the predicted AGB: $100 \times (0.5 \times 95\% \text{ confidence interval of the mean}) / \text{predicted AGB}$.

In general the uncertainty is low: 80.32% of the mapped area has an uncertainty less than 20%, and 10.2% of the mapped area has an uncertainty between 20% and 30%. Because it is a relative uncertainty, it is highest in the driest areas, which have a low predicted biomass.



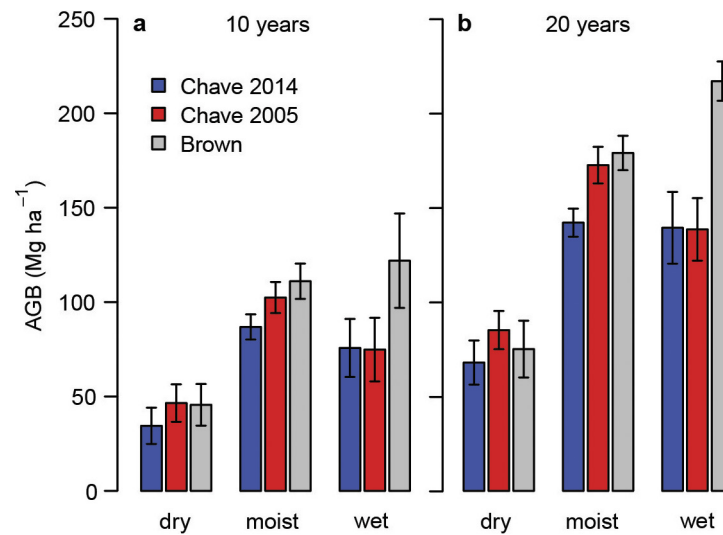
Extended Data Figure 4 | Relationship between forest biomass and stand age using chronosequence studies in Neotropical secondary forest sites. a, AGB ($N = 44$); b, AGB recovery ($N = 28$). The same as Fig. 1 but with plots and regression lines coloured by forest type: green, dry forest (<1,500 mm rainfall per year); light blue, moist forest (1,500–2,499 mm yr⁻¹); dark blue, wet forest (≥2,500 mm yr⁻¹). Each line represents a different chronosequence. The original plots on which the

regression lines are based are shown ($N = 1,364$ for AGB, $N = 995$ for AGB recovery). AGB recovery is defined as the AGB of the secondary forest plot compared with the median AGB of old-growth forest plots in the area, multiplied by 100. Significant relations (two-sided $P \leq 0.05$) are indicated by continuous lines, non-significant relationships (two-sided $P > 0.05$) are indicated by broken lines. Plots of 100 years old are also second-growth.



Extended Data Figure 5 | Potential biomass recovery map of Neotropical secondary forests. The same as Fig. 3 but with colour-blind-friendly colour coding. The total potential AGB accumulation over 20 years of lowland secondary forest growth was calculated on the basis of a regression equation relating AGB with annual rainfall ($AGB = 135.17 - 103,950 \times 1/rainfall + 1.522 \times rainfall$

seasonality + 0.1148 × CWD; see Methods). The colour indicates the amount of forest cover recovery (purple, low recovery; green, high recovery). The 44 study sites are indicated by circles; the size of the symbols scales with the AGB attained after 20 years. The grey areas do not belong to the tropical forest biome. The map focuses on lowland tropical forest (altitude <1,000 m).



Extended Data Figure 6 | AGB of secondary forest. a, AGB 10 years and b, 20 years after land abandonment. Predicted mean AGB is given for three different forest types (dry (<1,500 mm rainfall), moist (1,500–2,499 mm),

wet (≥2,500 mm)) using three different allometric equations (indicated by different colours). These allometric equations are ordered from left to right as ref. 34 (blue), ref. 33 (red), and ref. 32 (grey). Means ± s.e.m. are shown.

Extended Data Table 1 | Overview of the sites included in the study

Site	Country	Lat.	Long.	Rainfall	CWD	RS	CEC	FC	LU	AGB	%AGB	Age	Ref.
Bolpebra	Bolivia	-11.44	-69.16	1800	-301	55	6.4	80	SC	193.2	63.5	4-47	44
El Tigre	Bolivia	-11.98	-65.72	1780	-375	66	5.8	90	SC	145.0	32.3	3-25	45
El Turi	Bolivia	-11.75	-67.33	1833	-288	58	5.8	95	SC	129.4	47.8	2-40	45
Salvatierra	Bolivia	-15.50	-63.03	1200	-642	61	4.0	70	SC	38.3	29.5	1-36	46
San Lorenzo	Bolivia	-16.70	-61.87	1129	-718	59	4.5	40	SC	82.8	64.5	3-50	47
Surutu 1	Bolivia	-17.50	-63.50	1600	-496	54	6.1	45	SC	60.5	-	4-20	48
Surutu 2	Bolivia	-17.50	-63.50	1600	-496	54	6.1	45	SC	154.3	-	6-25	48
Bahia	Brazil	-14.48	-39.09	2000	-7	17	6.6	80	SC	96.7	25.4	10-40	49
Cajueiro	Brazil	-14.98	-43.90	840	-907	96	13.8	80	PA	52.2	-	15-59	
Serra do Cipo	Brazil	-19.35	-43.62	1519	-341	86	5.4	60	PA	130.3	-	8-50	
Eastern Pará 1	Brazil	-4.26	-47.73	1898	-548	88	7.8	50	SC & PA	168.2	-	5-25	50
Eastern Pará 2	Brazil	-2.16	-47.38	2460	-274	64	4.6	52	SC & PA	224.7	-	5-40	50
Eastern Pará 3	Brazil	-1.17	-47.75	2785	-306	68	4.3	58	PA	176.5	-	2-70	50
Manaus (<i>Cecropia</i> pathway)	Brazil	-2.35	-60.00	2400	-16	32	2.0	100	SC	181.2	55.8	5-31	51
Manaus (<i>Vismia</i> pathway)	Brazil	-2.35	-60.00	2400	-16	32	2.0	100	PA	140.6	43.3	2-25	51
Mata Seca	Brazil	-14.86	-43.99	825	-914	95	3.5	80	PA	58.8	-	14-58	52
Patos	Brazil	-7.02	-37.25	750	-1276	116	11.2	60	SC & PA	20.3	-	22-64	53
Rio Madeira (anthropogenic soil)	Brazil	-5.77	-61.43	2507	-109	46	3.4	79	SC	187.9	74.4	5-30	54
Rio Madeira (oxisol)	Brazil	-5.77	-61.43	2507	-109	46	4.7	79	SC	159.2	56.2	6.5-30	54
Sao Paulo	Brazil	-22.32	-47.57	1367	-297	72	10.2	31	PA	123.2	35.7	11-45	
Aracuara	Colombia	-0.60	-72.37	3059	-13	29	9.7	95	SC	134.5	39.2	2-30	55
Providencia Island	Colombia	13.35	-81.35	1584			31.8	60	SC & PA	135.9	-	6-56	56
San Carlos	Colombia	1.93	-67.05	3565	0	23	5.8	80	SC	84.6	35.5	9-80	57
Santa Rosa (oak forest)	Costa Rica	10.89	-85.60	1765	-608	91	32.4	70	PA	161.3	-	5-70	58
Palo Verde	Costa Rica	10.36	-85.31	1444	-622	88	39.0	70	PA	142.9	-	7-60	58
Santa Rosa	Costa Rica	10.86	-85.61	1765	-621	93	32.4	70	PA	170.9	84.9	6-70	58
Sarapiquí (Chazdon)	Costa Rica	10.43	-83.98	4000	0	29	29.0	77	PA	171.5	59.6	10-41	59
Sarapiquí (Letcher)	Costa Rica	10.43	-83.98	4000	0	29	29.0	77	PA	145.4	76.6	10-42	60
Chajul	Mexico	16.07	-90.75	3000	-248	62	10.8	50	SC	105.3	59.4	0-27	61
Chamela	Mexico	19.50	-105.05	788	-905	109	21.0	60	PA	34.8	49.9	3-15	62
Chinantla	Mexico	17.75	-96.65	3700	-596	83	10.1	95	SC	155.7	63.8	5-50	
El Ocote 1	Mexico	16.96	-93.63	1500	-558	69	26.3	80	SC	101.4	33.6	2-75	63
El Ocote 2	Mexico	16.96	-93.63	2000	-558	69	18.6	80	SC	116.4	62.3	3-75	63
Lacandona	Mexico	16.54	-90.96	2500	-325	68	37.0	87	SC & PA	206.3	-	1-31	
Marqués de Comillas	Mexico	16.33	-90.67	2250			21.4	49	SC & PA	206.3	-	2-50	
Nizanda	Mexico	16.66	-95.01	878	-1036	102	30.6	64	SC	34.7	25.4	2-60	64
Quintana Roo	Mexico	19.31	-88.57	1250	-508	54	64.6	85	SC & PA	90.0	66.4	2-100	
Yucatán	Mexico	20.08	-89.55	1100	-601	65	39.9	94	SC	69.3	66.7	3-70	65
Zona Norte	Mexico	17.27	-91.66	2750	-213	56	37.0	67	SC & PA	85.6	-	2-52	
Agua Salud	Panama	9.22	-79.78	2700	-326	57	9.3	70	SC & PA	81.8	-	2-31	66
Barro Colorado Island	Panama	9.15	-79.85	2600	-319	57	9.3	100	SC & PA	120.5	59.3	20-100	67
Pucallpa	Peru	-8.50	-74.80	1570	-56	34	21.4	43	SC & PA	99.2	-	5-30	
Cayey	Puerto Rico	18.02	-66.08	2000	-220	41	23.9	50	PA	110.5	61.8	10-80	68
El Carite	Puerto Rico	18.08	-66.07	1822	-165	35	20.5	71	PA	127.7	66.7	4-77	69
Luquillo	Puerto Rico	18.34	-65.76	2660	-12	31	9.5	75	PA	150.1	67.8	9-76	69

An overview of the name, country, latitude (Lat.) and longitude (Long.), rainfall (in millimetres), rainfall seasonality (RS), CWD (in mm per year), CEC (in centimoles of positive charge per kilogram of soil), percentage forest cover in the landscape matrix (FC; as a percentage), prior land use (LU: SC, shifting cultivation; SC & PA, some plots shifting cultivation, some plots pasture; PA, pasture), AGB (in megagrams per hectare) after 20 years, relative biomass recovery after 20 years (%AGB, as a percentage), the minimum and maximum secondary forest age (in years) included in the chronosequence, and a reference (refs 44–69) for each site is given.

Extended Data Table 2 | Overview of the modelling results of absolute ($N=43$, one site was excluded because of missing climatic data) and relative ($N=28$) AGB recovery after 20 years in relation to rainfall, CEC, land use, and forest cover in the landscape matrix

Variable	Model	ΔAIC_c	R^2
AGB at 20 yr (Mg/ha)	1/rainfall + CWD + Rainfall seasonality	0.00	0.59
AGB at 20 yr (%)	1/rainfall + CEC	0.00	0.23
	1/rainfall + CEC + Rainfall seasonality	1.53	0.27

All models within two AIC_c units of the best model are given. The change in AIC for small sample sizes compared with the best model (ΔAIC_c) and R^2 are given.